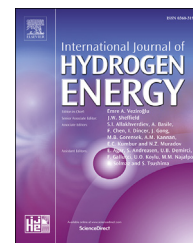


Available online at www.sciencedirect.com

ScienceDirect

journal homepage: www.elsevier.com/locate/he

Comparative genomic analysis of two heat-resistant *Rhodobacter capsulatus* mutants with different hydrogen production levels reveals mutations related to hydrogen production

Abdilmecit Gökçe^{a,b,c}, Yavuz Öztürk^{d,1}, Zeynep Petek Çakar^{a,b,*}

^a Department of Molecular Biology and Genetics, Faculty of Science & Letters, Istanbul Technical University, 34469 Maslak, Istanbul, Turkey

^b Istanbul Technical University, Dr. Orhan Öcalgiray Molecular Biology, Biotechnology & Genetics Research Center, ITU-MOBGAM, 34469 Maslak, Istanbul, Turkey

^c Department of Molecular Biology and Genetics, Faculty of Engineering and Natural Sciences, Bahcesehir University, 34353 Besiktas, Istanbul, Turkey

^d TÜBİTAK Research Institute for Genetic Engineering and Biotechnology, Kocaeli 41470, Turkey

ARTICLE INFO

Article history:

Received 22 April 2017

Received in revised form

15 June 2017

Accepted 1 July 2017

Available online 19 July 2017

Keywords:

Next generation sequencing

Biohydrogen

Bacterial genomics

Purple nonsulfur bacteria

PII uridylyl-transferase

ABSTRACT

To overcome efficiency losses due to overheating in outdoor photobioreactors for microbial hydrogen production, heat-resistant microorganisms are desirable. In this study, the comparative whole genome sequencing analyses of two previously obtained *Rhodobacter capsulatus* heat-resistant mutants; A52 and B41, with modified hydrogen production capacities, have been performed to identify mutations related to hydrogen production. In comparison with the reference strain DSM1710, the genomes of the mutants A52 and B41 contained 2137 and 2253 mutations, respectively. In the mutant B41 genome, mutations were characterized within the *nifD*, *nifJ*, *glnD*, *nifB1*, *ccpA*, *hupD*, *dmsA*, and *cbbR1* genes. On the other hand; in the A52 mutant, mutations were characterized in the *nifB2*, *mifF*, *nifJ*, *cbbO*, *anfH*, *amt*, *moeA*, and *hupD* genes. The effects of nitrogen metabolism and redox-related mutations were tested by quantitative reverse transcription PCR. The most promising mutation was found on the *glnD* gene of B41 strain with higher hydrogen production capacity.

© 2017 Hydrogen Energy Publications LLC. Published by Elsevier Ltd. All rights reserved.

Abbreviations: Hydrogen, H₂; Nitrogen, N; Quantitative reverse transcription polymerase chain reaction, qRT-PCR; Next generation sequencing, NGS; Calvin–Benson–Bassham cycle, CBB cycle; 1,5-bisphosphate carboxylase/oxygenase, RubisCO; Dimethyl sulfoxide, DMSO; Dimethyl sulfoxide reductase, DMSOR; Purple nonsulfur bacteria, PNS bacteria; Nitrogen regulation system, Ntr; The uridylyl transferase/uridylyl-removing enzyme, GlnD; Uptake hydrogenase, Hup.

* Corresponding author. Department of Molecular Biology and Genetics, Faculty of Science & Letters, Istanbul Technical University, 34469 Maslak, Istanbul, Turkey.

E-mail address: cakarp@itu.edu.tr (Z.P. Çakar).

¹ Present address: 1855 sk., No:10, D:5, 41180, Beşevler, Gebze, Kocaeli, Turkey.

<http://dx.doi.org/10.1016/j.ijhydene.2017.07.005>

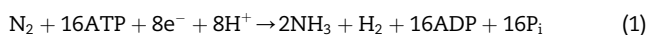
0360-3199/© 2017 Hydrogen Energy Publications LLC. Published by Elsevier Ltd. All rights reserved.

Introduction

Unhindered population growth, the impending shortage of energy resources and environmental problems emerging from the use of fossil fuels are leading the scientists to search for alternative energy sources, including wind, solar and biomass energy, and hydrogen (H_2) production [1]. Majority of the H_2 , nowadays, is being produced through physicochemical methods that involve the use of conventional energy sources such as (i) steam reforming of natural gas, (ii) partial oxidation of hydrocarbons, and (iii) coal gasification; or through the use of renewable energy sources like (i) solar photovoltaic power for direct conversion, (ii) wind power, and (iii) hydropower [2]. However, the most promising way of obtaining renewable energy is the production of H_2 using photosynthetic microorganisms such as algae or purple nonsulfur (PNS) bacteria [3]; since the generation of H_2 through photosynthesis has several advantages such as zero emission of greenhouse gases and other environmental pollutants, and production at ambient temperatures with minimal energy consumption [4,5].

Rhodobacter capsulatus is a PNS photosynthetic alpha-proteobacterium which is known for its metabolic plasticity enabling it to thrive in disparate ecological niches [6,7]. This feature of *R. capsulatus* makes it an ideal model for the study of respiratory, photosynthetic and chemolithotrophic growth modes [6–8]. For the last two decades, *R. capsulatus* particularly stands out for its ability to produce H_2 under nitrogen limiting conditions by using simple organic acids, such as acetic acid, lactic acid, malate, and butyrate as the carbon source [7–9].

The major route for H_2 production in *R. capsulatus* is the nitrogen fixation [6]. This process is catalyzed by the nitrogenase enzyme, by which H_2 is produced as a byproduct to enable cells to synthesize ammonia from nitrogen gas [10,11].



Since the nitrogen fixation process is highly energy-demanding, nitrogenase expression is strictly regulated at three different levels (Fig. 1) influenced by environmental factors such as availability of ammonium, light and the presence of oxygen [12].

At the first level of regulation (Fig. 1A), ammonium availability directs the Ntr system which controls the transcription of *nifA* and *anfA* genes, activators of all nitrogenase encoding genes [12]. Ntr system comprises five proteins: GlnD, the uridylyl transferase/uridylyl-removing enzyme; GlnB, the signal transduction protein (PII); GlnK, a PII paralogue; and two component response regulators NtrB and NtrC. Under nitrogen-limited conditions, PII is uridylylated by GlnD which can sense the nitrogen status of the cell by glutamine/2-ketoglutarate ratio [13]. When uridylylated, PII can no longer interact with NtrB, allowing NtrB to phosphorylate the NtrC response regulator. Phosphorylated NtrC (NtrC-P) activates the expression of its target genes including *nifA*, *anfA*, *glnK* and ammonium transporters *amtB* and *amtY*. At the second level (Fig. 1B), post-translational activity control of NifA is regulated by GlnB and GlnK [11]. In the presence of ammonium, GlnB and GlnK regulate the activity of NifA to repress the

expression of *nif* genes [12]. At the third level (Fig. 1C), GlnB, GlnK and ammonium transporters *AmtB* and *AmtY* regulate the nitrogenase reductase (NifH and AnfH) activity through reversible ADP-ribosylation in response to ammonium availability or light intensity. In the presence of ammonium, the nitrogenase reductase components of two alternative nitrogenases are ADP-ribosylated, and nitrogenase activity is reduced substantially [10].

Although the H_2 production in *R. capsulatus* is the product of nitrogenase driven N_2 assimilation, the rate of H_2 production is not just affected by this mechanism but also affected by other redox balancing systems which are competing for the electrons. The initial mechanism which maintains the intracellular redox balance in PNS bacteria is the CBB cycle when cells are cultured photoheterotrophically. However, specific conditions such as N_2 limitation and the presence of DMSO as an electron acceptor drives the alternative redox balancing systems; the nitrogenase and DMSOR, respectively [14]. It has been reported that the CBB-deficient mutant strains of *R. capsulatus* derepress the synthesis of the dinitrogenase system, and the H_2 production enhances [15]. However, in the presence of DMSO, the derepression of dinitrogenase protein accumulation or *nifH* promoter activity is severely diminished [15] due to sharing of electrons between nitrogenase and DMSOR systems.

To produce biohydrogen at industrial scale; a number of different photobioreactors have been designed, with differing sources of illumination [16]. Indoor photobioreactors require artificial illumination for H_2 production, while outdoor photobioreactors have the advantage of using the sun as the light source. However, it is impossible to control environmental conditions such as temperature in the outdoor photobioreactors [17]. In order to achieve a sustainable H_2 production in outdoor photobioreactors, two heat-resistant mutant strains (A52 and B41) of *R. capsulatus* were previously developed by our group through a directed evolution approach [16]. According to total H_2 production; A52 strain produces 7% less and B41 strain produces 24% more H_2 , compared to the wild-type strain DSM1710 [16] from which both strains were derived. The substrate conversion efficiencies of the mutant strains are 20.16% and 26.73% for A52 and B41 strains, respectively. The hydrogen yield of the A52 and B41 mutant strains are 1.21 and 1.61 mol H_2 /mol malate, respectively (Table 1).

In this study, comparative genomic analysis of two heat-resistant mutant strains of *R. capsulatus* (A52 and B41) with different H_2 production levels was conducted in order to determine which mutations affect H_2 production metabolism. In addition to genomic analysis, expression levels of critical genes with mutations were determined, including nitrogen fixation (*nif*) genes, *nifA*, *ntrC*, and *nifH*; RubisCO structural genes *cbhL*, *cbhS* and *cbhO*; PII uridylyl-transferase-encoding gene *glnD*; nitrogenase iron protein-encoding gene *anfH*; hydrogenase maturation protease-encoding *hupD*; molybdopterin biosynthesis protein-encoding *moeA*; ammonium transporter gene *amt*; and dimethyl sulfoxide reductase A subunit-encoding *dmsA* genes. Mutations affecting *cbhR1*, *dmsA*, and *glnD* were proposed as critical mutations which possibly changed the hydrogen production profiles of the mutants.

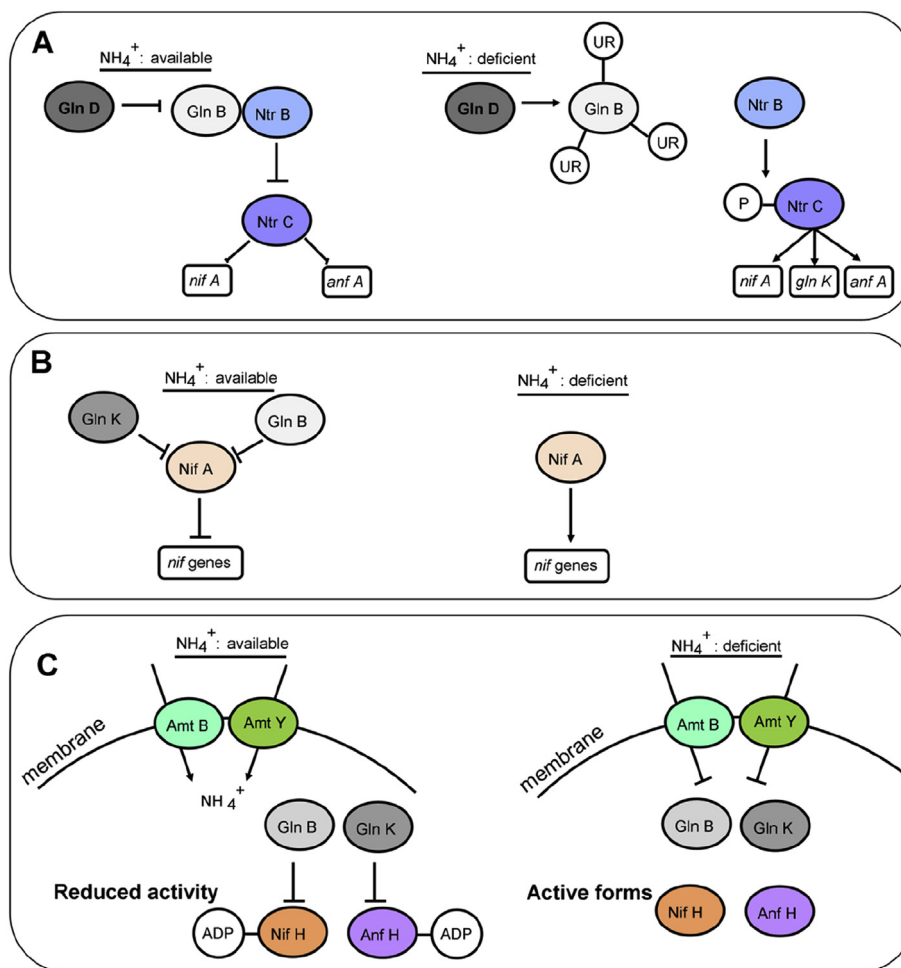


Fig. 1 – The schematic representation of nitrogen metabolism regulation in *R. capsulatus*; A) The first level of regulation in which GlnD regulates the PII protein GlnB whose function is to bind to NtrC and repress the expression of *nif* genes through uridylation and deuridylation depending on the availability of ammonium, B) The second level of regulation in which PII proteins are repressing the NifA-driven *nif* gene expression depending on ammonium availability, C) The third level of regulation in which ammonium transporters and PII proteins are controlling nitrogenase activity through ribosylation depending on ammonium in the environment.

Table 1 – List of *R. capsulatus* strains used in this study with their key phenotypic characteristics.

Strain	Description	Phenotype	Reference
DSM1710	Wild-type laboratory strain	Sensitive to 42 °C, Total H ₂ production 0.440 ± 0.009 ml/ml culture Substrate conversion efficiency (%) 21.60 ± 0.450 Hydrogen yield 1.31 mol H ₂ /mol malate	[6]
A52	Mutant derived from DSM1710 by directed evolution	Resistant to 42 °C, Total H ₂ production 0.407 ± 0.017 ml/ml culture Substrate conversion efficiency (%) 20.16 ± 0.851 Hydrogen yield 1.21 mol H ₂ /mol malate	[16]
B41	Mutant derived from DSM1710 by directed evolution	Resistant to 42 °C, Total H ₂ production 0.540 ± 0.018 ml/ml culture Substrate conversion efficiency (%) 26.73 ± 0.930 Hydrogen yield 1.61 mol H ₂ /mol malate	[16]

Materials and methods

Strains and growth conditions

The bacterial strains used in this study are listed in Table 1. *R. capsulatus* strains were grown on MPYE (magnesium–calcium, peptone, yeast extract) enriched medium [7] and the minimal medium of Biebl and Pfennig supplemented with Carbon/Nitrogen (C/N) sources (15 mM malate/2 mM L-glutamate) [9]. Photosynthetic cultures were incubated at 34 °C, in anaerobic jars with H₂ and CO₂-generating gas packs (BBL 270304, Becton Dickinson and Inc) under saturating light intensity (around 3000 lux) provided by two 75-W tungsten lamps, which were placed next to the anaerobic jars.

Isolation of genomic DNA

Cultures of the *R. capsulatus* wild-type strain DSM1710 and the mutants A52 and B41 were grown in 10 mL MPYE-rich medium with shaking (100 rpm) for 2 days and harvested by centrifugation at 2800g for 20 min, washed with 10 mM Tris·HCl buffer at pH 8.0 and frozen at –20 °C overnight. Genomic DNA was isolated using the Invitrogen Genomic DNA Extraction Kit. The concentration and purity of isolated genomic DNA were determined on a Nano Drop2000 microvolume spectrophotometer (Thermo Fisher).

Genome sequencing and analysis

Genomes of *R. capsulatus* DSM1710 strain and the mutants A52 and B41 were sequenced on an Illumina HiSeq2000 genome sequencer. Genomic DNA libraries with insert size between 200 and 300 bp were prepared by using Illumina TrueSeq DNA sample prep kit for paired-end sequencing, according to the manufacturer's instructions (Illumina Inc.). The resulting genomic DNA libraries were sequenced to yield 12 to 15 million reads of 100-bp length. Illumina standard quality check and filtering conditions were used. For each analyzed genome, the reads were mapped to the reference genome of *R. capsulatus* SB1003 strain, available in GenBank (GenBank accession no. CP001312.1 and CP001313.1) using the Breseq platform [18] which reports single-nucleotide mutations, point insertions and deletions, large deletions, and new junctions supported by mosaic reads (such as those produced by new mobile element insertions) in an annotated HTML format. Sequence reads obtained with the wild-type laboratory strain DSM1710 were aligned against the *R. capsulatus* SB1003 reference genome, and the SNPs and INDELs that it contained were defined. Yet the variants originated from each mutant strain were compared to the variants of wild-type DSM1710 strain with gdttools, which is found in the Breseq pipeline, to be able to decide important variations between the mutants and the wild-type DSM1710 strain. Sequence reads for the mutants have been deposited in NCBI Sequence Read Archive with the following accession numbers; SRR4294674 and SRR4294678 for A52 and B41 mutants, respectively. Draft genome assemblies of the mutants have been deposited in DDBJ/EMBL/GenBank under the accession numbers LLVU00000000 and LLVV00000000 for B41 and A52, respectively [19].

qRT-PCR analyses

An amount of culture corresponding to ~10⁹ cells was centrifuged at 500g for 5 min at 4 °C, and the cells were washed twice with ice-cold PBS buffer. Total RNA was isolated using the TRIzol® Reagent (Thermo Fisher) according to the manufacturer's instructions. 100 ng of RNA was used for RT-PCR reaction with the SuperScript® III One-Step RT-PCR System (Thermo Fisher). A reaction mixture consisted of 5 µl reaction buffer, 0.1 nmol of each appropriate primer (Table 2), 1 µl of enzyme mix (reverse transcriptase and DNA polymerase) and ddH₂O up to 25 µl. All samples were run in triplicate for the target genes *nifH*, *nifA*, *ntrC*, *anfH*, *hupD*, *glnD*, *cbbL*, *cbbS*, *cbbO*, *dmsA*, *moeA*, *amt*, and the reference gene *rpoZ* (a housekeeping σ -factor). Relative expression levels were normalized with respect to the reference housekeeping gene, and quantification analysis was carried out by qBase method [20].

Reproducibility and statistical analysis

All results presented in this work are the average of three biological replicates. The significance was reported at $P < 0.01$ for qRT-PCR results. All statistical analyses were performed by using Minitab®15, software for statistics and BIORAD CFX Manager™ Software.

Results and discussion

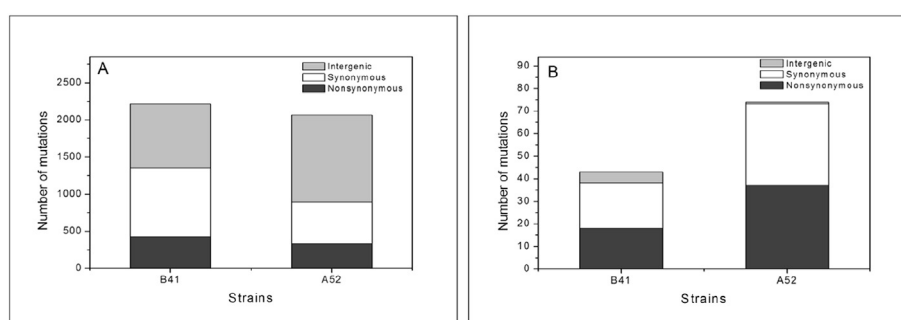
Comparative genomic analyses of wild-type and mutant *R. capsulatus* strains

In comparison with the reference strain DSM1710, the genome of mutant A52 contains 2137 mutations, 2063 of which are chromosomal (Fig. 2A and S1 Table). The genome of mutant B41 has 2253 mutations (including 2220 in the chromosome) compared to the reference strain DSM1710 (Fig. 2A and S2 Table). A number of mutations, 43 in B41 and 74 in A52, were found on the pRCB133 plasmid, however; since the coverage of plasmid DNA with the A52 sequencing reads were low for some regions (~5 coverage), we did not focus on the pRCB133 plasmid which has a very limited number of genes related to H₂ production metabolism (Fig. 2B).

The genomes of the strains A52 and B41 contain missense and nonsense mutations on 309 and 330 putative genes, respectively. Those putative genes include those possibly encoding proteins of unknown function, membrane transporters, membrane receptors, signal transduction kinases, stress response proteins, DNA repair proteins, and nitrogen-related genes for both mutants. It should be noted that A52 and B41 are derived from the same batch of the DSM1710 culture to which chemical mutagenesis and directed evolution were applied to obtain heat-resistant strains of *R. capsulatus* [16]. Since both mutant strains are heat-resistant, it is not surprising to observe that many mutations were induced on the same genes. These mutations on the corresponding shared genes are most likely related to heat resistance. On the other hand, the mutations that are specific to each strain are probably related to the hydrogen production metabolism of *R. capsulatus*, mutant strains.

Table 2 – List of primers used in this study.

Gene	Forward primer	Reverse primer
<i>nifH</i>	5'- GTGTCCTATGACGTTCTGGGCGACG-3'	5'- CCGCCCAGACGACGCGCCCGAG-3'
<i>nifA</i>	5'- CGGTTACGCAGTTTTCAG-3'	5'- AGTTCGCGCGCATCTTTAT-3'
<i>ntrC</i>	5'- ATTACCTGCCCAAGCCCTTC-3'	5'- TGATCATCACCGGCAGATCG-3'
<i>rpoZ</i>	5'- ACCGCTTCGAGCTGGTGATGCTTC-3'	5'- CTCGATCTGGGTCTGGTTGCTTTCG-3'
<i>cbbL</i>	5'- GCGACATTCTGGCCGCTTC-3'	5'- TTGACGACCGAGCCTTCCTC-3'
<i>cbbS</i>	5'- ATCCGTCGTCAGGTCGAGTG-3'	5'- CATAGCCGATCAGCCGGACA-3'
<i>cbbO</i>	5'- ACGAGGTCGAGGTCGAAACC-3'	5'- CAAGATCGCCTCGGTGAGGT-3'
<i>hupD</i>	5'- GCGGTCGATTTCGGCTTCAC-3'	5'- CCGCCGTAATCCTCCAGCTC-3'
<i>dmsA</i>	5'- GACAGCAACCGATCAAGCG-3'	5'- GGTGAAGCGGGGAGATAGT-3'
<i>moeA</i>	5'- CGCATCACATCGGCCTTCTG-3'	5'- GATGCCGTGATCGTCGACCT-3'
<i>amt</i>	5'- CCTTGTTGCTGGCGGTGATG-3'	5'- ACATCCAGGACAGCGAAGCG-3'
<i>glnD</i>	5'- GACGAGATCCGCATCGACCT-3'	5'- AGTTTCGTGGCCTCGTAGGG-3'
<i>anfH</i>	5'- ATGCCGCCAACACATCTGC-3'	5'- CGGTACGGTCTGCTTGTG-3'

**Fig. 2 – Distribution of different types of mutations on chromosomal (A) and plasmid (B) DNA sequences for the mutant strains B41 and A52.**

Mutations that might affect hydrogen production metabolism

Different mutations, likely to be related to hydrogen production metabolism, have been determined on each of the mutant strains. The lists of the mutations are represented in [Tables 3 and 4](#).

The *nifD* gene whose product is the alpha chain of nitrogenase has a mutation in the B41 mutant on nitrogenase/oxidoreductase component I domain at position 226. B41 has a missense mutation in that position in which a threonine has been replaced by an asparagine (T226N) residue ([Table 3](#)) that is neither found in A52 mutant strain nor the wild-type DSM1710 strain. Since threonine and asparagine are both

polar and uncharged amino acids, the effect of this mutation on folding of the NifD protein would not be drastic. However, the size of asparagine is larger than that of threonine; thus, this mutation may enhance the formation of dimeric NifDE, component I of the nitrogenase, by increasing the interaction surface between subunits, and increase H_2 production.

Pyruvate-flavodoxin oxidoreductase encoded by the *nifH* gene is an accessory protein for nitrogen assimilation [21] and has two missense mutations on each mutant strain. A52 has A920E mutation, and B41 contains a mutation at position 966 in which a proline turned into an arginine (P966R) ([Table 3](#)). Both of these mutations reside on the thiamine diphosphate binding fold domain of NifH, which acts as an electron donor and reduces the flavodoxin and ferredoxin I in *R. capsulatus*

Table 3 – Mutations in the B41 genome that might be related to higher levels of H_2 production.

Gene	Gene product	Mutation type	Mutation
<i>nifD</i>	Nitrogenase molybdenum-iron protein alpha chain	Missense	T226 N
<i>nifH</i>	Pyruvate flavodoxin oxidoreductase	Missense	P966R
<i>glnD</i>	PII uridylyl-transferase	Missense, Intergenic	I911T, (-31) +10bp
<i>nifB1</i>	Nitrogenase cofactor biosynthesis protein NifB1	Missense	R469L
<i>ccpA</i>	Cytochrome c peroxidase	Missense	A17D, P402A, and K405T
<i>dmsA</i>	Dimethyl sulfoxide reductase, A subunit	Intergenic	-19, -25, -28 and -43
<i>hupD</i>	Hydrogenase maturation protease HupD	Intergenic	-200, -196, -194
<i>cbbR1</i>	RubisCO operon transcriptional regulator CbbR-1	Missense	T273H, S294G and G296E

Table 4 – Mutations in the A52 genome that might be related to decreased levels of H₂ production.

Gene	Gene product	Mutation type	Mutation
<i>nifB2</i>	Nitrogenase cofactor biosynthesis protein NifB2	Missense	H474Q
<i>rnfF</i>	Nitrogen fixation protein RnfF	Missense	R317T
<i>nifJ</i>	Pyruvate flavodoxin oxidoreductase	Missense	A920E
<i>cbbO</i>	RubisCO activation protein CbbO	Intergenic	(–4) +10bp
<i>anfH</i>	Nitrogenase iron protein	Intergenic	–210
<i>moeA</i>	Molybdopterin biosynthesis protein MoeA	Intergenic	–260, –255, –162, –147
<i>hupD</i>	Hydrogenase maturation protease HupD	Intergenic	(–196) Δ 1bp, –193, –187, –185
<i>amt</i>	Ammonium transporter	Intergenic	(+72) Δ 1bp

[22,23]. Both mutations reside on the interaction surface of the NifJ protein and its physiological electron acceptors (flavodoxin and ferredoxin I). The protein-protein interactions between the NifJ and electron acceptors might be affected positively in the case of P966R in the B41 mutant, and negatively in the case of A920E in the A52 mutant. Although the alignment analysis for NifJ showed that these residues are not conserved among the *Rhodobacter* genus, the effect of these mutations on the activity of NifJ may be critical.

The *glnD* gene, which encodes the bifunctional uridylyl-transferase (UTase)/uridylyl-removing (UR) enzyme, modifies PII regulatory proteins by uridylation and deuridylation in response to the nitrogen status of the cell [24]. At low glutamine level which is a sign of ammonium deprivation, GlnD protein catalyzes the conversion of PII protein into PII-UMP with UTase activity; while at high glutamine levels which indicate saturated ammonium level, GlnD hydrolyzes the PII-UMP to PII that prevents NifA from activating the transcription of *nif* genes [25]. In the mutant strain B41, the missense mutation (I911T) is on the C-terminal ACT domain (ACT2) that is the ligand binding site for glutamine (Table 3). Alignment analysis for GlnD proteins among *Rhodobacter* genus revealed that this residue is well conserved among *Rhodobacter* species. Deletion of ACT domains was reported to lower UR activity but not change the UTase activity of GlnD in *Escherichia coli* and *Rhodospirillum rubrum* [26]. When ACT domains are deleted, glutamine can no longer stimulate UR activity; therefore the repression of *nif* gene expression by UR activity will be suppressed. Thus, the constitutive *nif* expression could occur even when the amount of fixed nitrogen (in NH₄⁺ form) is increasing. This mutation may lead to the higher H₂ production in B41 by inhibiting the UR activity of the GlnD protein. There is an intergenic mutation which resides in the promoter region of the *glnD* gene in B41 mutant strain. It is at the position of –31 and 10 nucleotides have been added to that position (Table 3). –35 position is a critical position for the promoters and the insertion mutation in this region is likely to change the expression level of the GlnD protein drastically.

NifB is a homodimeric protein composed of two domains; the radical S-adenosyl-L-methionine (SAM) domain and dinitrogenase iron-molybdenum cofactor (FeMo-co) biosynthesis domain which is crucial for FeMo-co biosynthesis by supplying iron-sulfur clusters to the structure [27]. A missense mutation was determined on FeMo-co domain at position 469 (R469L) in B41 (Table 3). This position is highly conserved among *R. capsulatus* strains; however, in *Rhodobacter* genus, instead of the positively charged arginine, a nonpolar amino acid leucine is found with this missense mutation. It has been

reported that missense mutations on the *nifB* gene may result in the formation of unstable NifB proteins whose activity drops drastically [28]. Although there is no evidence about the effect of the R469L mutation, it can be speculated that the missense mutation may result in the formation of a more stable NifB protein, since the NifB amino acid sequence of B41 resembles those of other *Rhodobacter* species which have higher H₂ production levels compared to *R. capsulatus*. Thus, this mutation can be an important one for H₂ production and may lead to the higher hydrogen production in B41.

Cytochrome c peroxidase (*ccpA*) whose main function is to detoxify the hydrogen peroxide (H₂O₂), which is generated due to over-reduction of the membrane-bound electron transfer chain, into water [29], got mutated (A17D) in B41 (Table 3). The missense mutation was found on the signal peptide and it is an effective mutation where the nonpolar amino acid turned into a negatively charged residue. The cytochrome c peroxidase is first synthesized as a pro-apo-cytochrome that is translocated across the cell membrane where the signal peptide is cleaved and cytochrome c peroxidase is attached in the periplasm [30]. The mutation on the signal peptide may affect the localization in periplasm where it is functional. There are also two missense mutations on di-haem-cyt-c peroxidase domain of *ccpA* (P402A and K405T) which are specific to B41 (Table 3). Cytochrome c peroxidase detoxifies the H₂O₂ with the electrons supplied by its counterpart cytochrome c [31] whose deletion in *R. capsulatus* resulted in lower H₂ production by affecting the efficiency of photosynthesis and peroxidase activity [7]. Due to the missense mutations, electron transfer from cytochrome c to cytochrome c peroxidase might have been inhibited such that the electrons could be used for H₂ production. Thus, these mutations might have increased the H₂ production levels in B41.

Many bacteria can grow anaerobically by using DMSO as the terminal electron acceptor. Also under photoheterotrophic growth conditions, over-reduced ubiquinol pool is reduced through the DMSOR system in the presence of DMSO or the reduction of protons into H₂ by nitrogenase to maintain redox balance in *R. capsulatus* [32]. Thus, DMSOR and nitrogenase are competing with each other in the presence of DMSO in the medium. The mutations in the promoter region of the DMSOR-encoding gene *dmsA* (at positions –19, –25, –28 and –43) in B41 (Table 3) might be important for the regulation of DMSOR synthesis. However, as the hydrogen production of the mutants was tested in BP medium without DMSO [16], the observed differences between their hydrogen production levels cannot be related to the mutations of the DMSOR system.

The *cbbR1* gene which is the master regulator for microbial CO₂ fixation [33] has three point mutations on the LysR substrate binding domain. This domain includes a DNA binding motif, which makes the CbbR bind to the promoter of *cbb* genes to activate them. Thus, the mutations in the LysR substrate binding domain may lead to a change in the expression levels of *cbb* genes. In the presence of fixed carbon sources, the primary role of the CBB cycle changes into facilitating the use of CO₂ as an electron sink by which CO₂ is being used as the terminal electron acceptor to balance redox homeostasis [34].

hup genes encode an uptake hydrogenase enzyme whose function is to recycle the H₂ which is produced by nitrogenase system. The *hupD* gene encodes the hydrogenase maturation protease which is involved in the formation of catalytically active uptake hydrogenase [35]. The comparative genomic analysis of B41 mutant strain revealed three intergenic mutations in the upstream region of the *hupD* gene. Similar to B41, there are four intergenic mutations in the upstream region of the *hupD* gene in the A52 mutant strain. However, they are different mutations than those found in B41. These mutations have the ability to change HupD gene expression, thus the ability of this mutant to synthesize active uptake hydrogenase enzyme. It has been reported that *hup*[−] strains of *R. capsulatus* exhibit higher hydrogen production capacity [7].

In the A52 strain, two missense mutations that are directly related to nitrogen metabolism have been found on *nifB2* (H474Q) and *mfF* (R317T) genes (Table 4). *nifB2* gene encodes the nitrogenase cofactor biosynthesis protein, and the mutation is on the dinitrogenase iron-molybdenum cofactor biosynthesis domain [36]. The missense mutation leads a positively charged amino acid (histidine) to change into a polar non-charged amino acid (glutamine) which could disrupt the biosynthesis of the iron-molybdenum cofactor. This mutation could downregulate the nitrogenase expression in A52. Yet another missense mutation has been characterized on the *mfF* gene of A52 strain which encodes the nitrogen fixation protein RnfF. The *rnf* genes of *R. capsulatus* are essential for nitrogen fixation, as they encode a system for electron transfer to nitrogenase [37]. The *mfF* gene product is an electron transporter which does not resemble any other electron transporter protein [38]. The missense mutation is on the ApeE like domain which is a Mg²⁺-dependent flavin mononucleotide to a threonine residue in bacterial flavoproteins [39]. Thus, the mutation may inhibit the electron transfer ability of RnfF which may lower the nitrogenase activity [38]. Therefore, the mutation on *mfF* gene seems to be crucial for decreased H₂ production in A52.

Besides the missense mutations, a number of mutations have been determined in the A52 mutant in the intergenic regions of RubisCO activation protein-encoding *cbbO*, nitrogenase iron protein-encoding *anfH*, molybdopterin biosynthesis protein-encoding *moeA*, hydrogenase maturation protease-encoding *hupD*, and ammonium transporter-encoding *amt* genes.

The CbbO protein has a well-defined function in the activation of RubisCO with its partner CbbQ [40]. Mutational analysis of *cbbO* gene revealed that CbbO protein acts as a substrate adaptor which binds to RubisCO, and CbbQ functions as a motor to activate RubisCO in order to maximize CO₂

fixation [41]. In A52, the intergenic mutation at the promoter region of the *cbbO* gene is a 10 bp long insertion which is most likely going to change the expression of the *cbbO* gene, and thus the activity of RubisCO. As explained earlier, the change in the activity of RubisCO affects the hydrogen production due to electron flux redirection to nitrogenase system [34].

The *anfH* gene is one of the structural genes of alternative nitrogenase in *R. capsulatus* [42]. The intergenic mutation in the upstream region (−210) of the *anfH* gene in A52 could possibly change the expression level of nitrogenase structural protein AnfH by which H₂ production may alternate.

The molybdenum cofactor is essential for enzymes like nitrogenase which are involved in important redox reactions in the global carbon and nitrogen cycles. The molybdenum cofactor synthesis takes place in three steps. In the third step, molybdate is inserted to the molybdopterin in a reaction catalyzed by MogA and MoeA. MoeA mediates molybdenum ligation, whereas MogA helps facilitate this step in an ATP-dependent manner [43]. In A52, we identified four intergenic mutations (−260, −255, −162 and −147) in the upstream region of the *moeA* gene that encodes molybdopterin biosynthesis protein MoeA. These intergenic mutations may change the expression of MoeA protein and may lead to a change in the amount of active molybdopterins which are crucial for nitrogenase function.

Ammonium transporters are important for the regulation of *nif* genes expression and the activity of nitrogenases (Fig. 1) [44]. Although we did not detect any mutation on *amtB* and *amtY* genes which have well-known regulatory functions on nitrogenase activity, the *amt* gene which encodes an alternative membrane ammonium transporter has a mutation in the intergenic region (+72, Δ1bp) of A52. This mutation could change the expression level of ammonium transporter, and may thus lead to a change in H₂ production.

To sum up, the analysis of the mutant strain genomes has revealed several mutations which are possibly related to changes in H₂ production levels. The most promising mutations involve the *glnD*, *nifB*, *nifJ* and *dmsA* genes of B41; and the *rnfF*, *anfH*, *moeA*, and *amt* genes of the A52 strain.

The effects of the mutations on the expression levels of genes involved in nitrogen metabolism and alternative redox balancing systems

As mentioned in Section Mutations that might affect hydrogen production metabolism, GlnD is a critical protein which can sense the nitrogen status of the cell and activates or deactivates GlnB through uridylylation or deuridylylation to enhance or repress *nif* gene expression through NifA in *R. capsulatus* [45]. Thus, to understand the effects of intergenic and ACT2 domain mutations on the *glnD* gene of the B41 strain, the expression levels of the genes encoding regulatory proteins - NifA, NtrC, and the nitrogenase structural proteins- NifH and AnfH were determined in the mutant strains under photoheterotrophic and nitrogen-limited conditions, using qRT-PCR.

qRT-PCR results showed that the expression levels of *nifA* and *nifH* genes decreased dramatically in A52, and increased by two-fold in B41, compared to the wild-type strain DSM1710. Additionally, alternative nitrogenase structural gene *anfH* was

50% less expressed in A52, while the expression of *anfH* was four-fold higher in B41 (Fig. 3). The increase in the *nifA* expression is directly corresponding with the increase in nitrogen fixation and H_2 production. Since the *nifA* gene product is a transcription factor which activates the expression of all *nif* genes, the increase in *nifH* and *anfH* expression is an expected result. The changes in expression levels of *nifA* and *nifH* are almost at the same level which implies that the change in *nifH* expression is directly related to the change in *nifA* gene expression. On the other hand, 50% reduction of the *anfH* gene expression in A52 may be directly related to the intergenic mutation on the *anfH* gene in this strain. The expression level of *ntrC* slightly decreased in both mutants, however, this decrease is statistically not significant ($p > 0.01$, Fig. 3). This result also coheres with the *glnD* mutation which does not have any effect on the expression level of the *ntrC*. However, the I911T mutation on the C-terminal ACT domain (ACT2) of GlnD may be lowering UR activity and results in more uridylylated GlnB (PII-UMP) which activates the *ntrC*. More active form of *ntrC* increases the expression levels of *nifA* and *anfA* genes that activate the nitrogenase genes (*nifH*, *anfH*) in B41 (Fig. 3). The *glnD* gene expression in A52 was almost at the same level with that of the wild-type DSM1710 strain and 7-fold less compared to the B41 which shows that the intergenic mutation (−31, +10bp) of the *glnD* gene in B41 enhances *glnD* gene expression. Enhanced GlnD production with lower UR activity could be the main reason for the higher H_2 production in B41.

Besides *glnD*, mutations on other nitrogen metabolism-related genes were also detected. In A52, two genes responsible for molybdopterin biosynthesis (*moeA*) and ammonium transfer (*amt*) have mutations in their intergenic regions. The *moeA* encodes an important protein for the synthesis of Mo–Fe nitrogenases. qRT-PCR analyses of this gene revealed that expression of *moeA* is downregulated in both mutant strains, however, the downregulation in B41 is not statistically significant ($p > 0.01$). The downregulation of *moeA* gene in A52 strain was about 13-fold, compared to the wild-type strain. This result is totally in agreement with the downregulation of *nifH* gene encoding the dinitrogenase component of Mo–Fe nitrogenase enzyme. The ammonium transporter *amt* gene expression analysis showed that ammonium transporter

expression was repressed in both mutants. Compared to the wild-type strain, the expression of *amt* was 12-fold and 7-fold lower in A52 and B41, respectively. Since the ammonium amount in the cell is the primary signal to retain nitrogen fixation, downregulation of ammonium transporter could be one of the factors affecting the H_2 production in both mutant strains.

In addition to mutations that affect the nitrogen metabolism, we also determined the gene expression levels of other redox balancing systems (Fig. 4), such as RubisCO, DMSO reductase and uptake hydrogenase systems, where their deletion is known to strongly enhance the H_2 production in *R. capsulatus* [7,32,46].

The *cbbR1* gene encodes the CbbR protein which is the activator of *cbb* (RubisCO) genes. The missense mutations found in this gene reside on the interaction surface of CbbR transcription factor and DNA [33,34]. Therefore, these mutations were proposed to change the expression of other *cbb* genes. The effect of these mutations was investigated by determining the expression levels of other *cbb* genes: *cbbL*, *cbbS*, and *cbbO*. The structural *cbb* genes, *cbbL*, and *cbbS* encode the large and small subunits of RubisCO, and *cbbO* is required for the expression of active RubisCO. qRT-PCR analyses showed that the expression of structural RubisCO genes was enhanced in B41 and repressed in A52, yet the changes are not statistically significant (Fig. 4, $p > 0.01$). *cbbO* gene expression, on the other hand, was found to be downregulated in both mutants by a factor of 10 (Fig. 4). These results showed that although the structural RubisCO genes were upregulated, due to *cbbO* repression, the synthesized RubisCO may have a lower activity in B41, compared to the wild-type strain. The lower activity of RubisCO could not be the main reason for the enhanced H_2 production in B41, but due to redox poise redirection to nitrogenase, it could contribute to higher H_2 production in the presence of elevated nitrogenase in this mutant.

In B41, we detected intergenic mutations (−19, −25, −28, −43) in the promoter region of *dmsA* gene which encodes the DMSOR. These mutations were thought to significantly change *dmsA* gene expression. qRT-PCR analyses showed that *dmsA* expression was repressed in both mutant strains. The *dmsA* expression in B41 was about 3-fold lower, and in A52

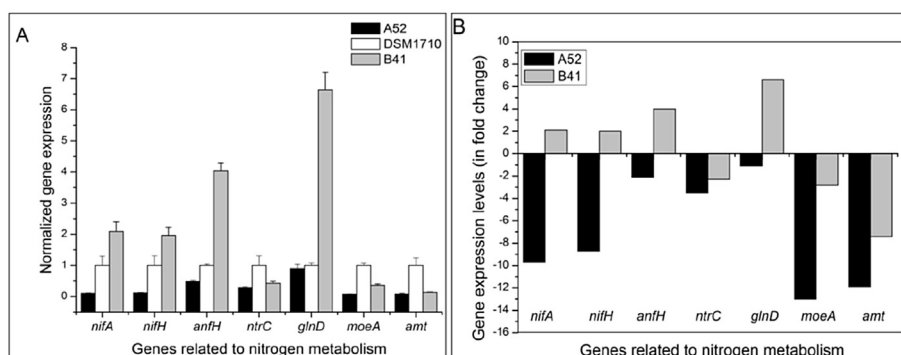


Fig. 3 – Expression levels of nitrogen metabolism-related genes *nifA*, *nifH*, *anfH*, *ntrC*, *amt*, *moeA*, and *glnD* in mutant strains A52 and B41; A) relative normalized gene expression values, B) fold-changes in gene expression. The values are normalized to those of the wild-type strain DSM1710. The qRT-PCR results represented here are the average of three biological replicates which were normalized with *rpoZ* expression.

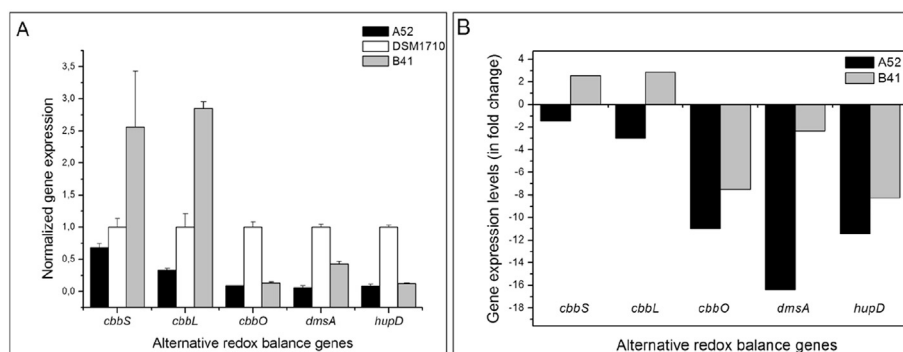


Fig. 4 – Expression levels of alternative redox balancing systems-related genes *cbbS*, *cbbL*, *cbbO*, *dmsA* and *hupD* in mutant strains A52 and B41; A) relative normalized gene expression values, B) fold-changes in gene expression. The values are normalized to those of the wild-type strain DSM1710. The qRT-PCR results represented here are the average of three biological replicates which were normalized with *rpoZ* expression.

16-fold lower, compared to the wild-type strain (Fig. 4). Although we did not expect to observe any *dmsA* gene expression change in A52, where no mutations associated with *dmsA* were detected, surprisingly, the level of repression in this mutant was even higher than the repression level in B41. These results imply that in A52, there should be mutations in other genes which control the expression of DMSOR.

Mutations were detected in the intergenic regions of the *hupD* gene in both mutant strains. The *hupD* gene encodes a protease which is required for the proteolytic cleavage of structural uptake hydrogenase proteins to create a catalytically active uptake hydrogenase whose function is to recycle the H_2 produced by nitrogenase [35]. The qRT-PCR results showed that *hupD* gene expression was repressed in both mutants by about 10-fold (Fig. 4). Since the uptake hydrogenase decreases the amount of H_2 produced from *R. capsulatus*, lower expression of HupD protein which will result in reduced activity of uptake hydrogenase will lead to higher H_2 production. Thus, the intergenic mutations on the *hupD* gene in B41 could be another reason for the enhanced hydrogen production in this strain. However, the decrease in *hupD* gene expression in A52 did not result in an increase in H_2 production because the expression of *nifA* and *nifH* genes were repressed nearly by 10-fold in A52.

The gene expression analyses together with the comparative genomic analyses imply that the mutations on the *glnD* gene which affect the expression of *nifA*, *anfH* and *nifH* genes; *cbbR1* mutations whose effect was observed especially on *cbbO* gene expression; *dmsA* mutation which is downregulating the DMSO reductase expression; and *hupD* mutations are the main reasons for the enhanced H_2 production in the B41 mutant strain. Besides, the mutations on *nifJ*, *rnfF* and especially *nifB2* might be the main reasons for the decreased H_2 production in the A52 mutant.

Conclusions

The comparative genomic analysis of heat-resistant *R. capsulatus* mutant strains revealed a number of missense and intergenic mutations which are related to hydrogen production metabolism. The mutant strain B41 with higher hydrogen

production levels has mutations on *nifD*, *nifJ*, and *nifB* nitrogen fixation genes, along with the genes encoding nitrogen fixation control elements (*glnD*), and redox-balancing proteins DMSOR (*dmsA*), uptake hydrogenase activator *hupD*, and cytochrome c peroxidase (*ccpA*). On the other hand; the mutant with lower hydrogen production capacity, A52, has mutations in four nitrogen fixation genes: *nifB2*, *rnfF*, *anfH*, and *nifJ*. The mutations on the *glnD* gene of B41 include a missense mutation and an insertion in the promoter region which we suggest as the most critical mutations, among all mutations that change the deuridylylation activity of GlnD and make the *nifA*, *nifH* and *anfH* expression higher, as supported by qRT-PCR analysis results.

Acknowledgements

This work was supported by the Scientific and Technological Research Council of Turkey (TUBITAK) [grant number 214Z138 (PI: Z. P. Cakar)]; Istanbul Technical University Research Funds for Ph.D. Thesis Projects [grant number 39572 (PI: Z. P. Cakar)]. Authors express their thanks to Bekir Ergüner, National Research Institute of Electronics and Cryptology, Advanced Genome & Bioinformatics Research Laboratory (TUBITAK), for the sequencing analyses.

Appendix A. Supplementary data

Supplementary data related to this article can be found at <http://dx.doi.org/10.1016/j.ijhydene.2017.07.005>.

REFERENCES

- [1] Antonopoulou G, Ntaikou I, Gavala HN, Skiadas IV, Angelopoulos K, Lyberatos G. Biohydrogen production from sweet sorghum biomass using mixed acidogenic cultures and pure cultures of *Ruminococcus albus*. *Glob Nest J* 2007;9:144–51.
- [2] Kothari R, Buddhi D, Sawhney RL. Comparison of environmental and economic aspects of various hydrogen

- production methods. *Renew Sust Energy Rev* 2008;12:553–63.
- [3] Voloshin RA, Rodionova MV, Zharmukhamedov SK, Veziroglu TN, Allakhverdiev SI. Review: biofuel production from plant and algal biomass. *Int J Hydrogen Energy* 2016;41:17257–73.
 - [4] Rodionova MV, Poudyal RS, Tiwari I, Voloshin RA, Zharmukhamedov SK, Nam HG, et al. Biofuel production: challenges and opportunities. *Int J Hydrogen Energy* 2017;42:8450–61.
 - [5] Azwar MY, Hussain MA, Abdul-Wahab AK. Development of biohydrogen production by photobiological, fermentation and electrochemical processes: a review. *Renew Sust Energy Rev* 2014;31:158–73.
 - [6] Imhoff JF. Taxonomy and physiology of phototrophic purple bacteria and green sulfur bacteria. In: Blankenship RE, Madigan MT, Bauer CE, editors. *Anoxygenic photosynthetic bacteria*. Dordrecht: Kluwer; 1995. p. 1–15.
 - [7] Öztürk Y, Yücel M, Daldal F, Mandacı S, Gündüz U, Türker L, et al. Hydrogen production by using *Rhodobacter capsulatus* mutants with genetically modified electron transfer chains. *Int J Hydrogen Energy* 2006;31:1545–52.
 - [8] Obeid J, Magnin JP, Flaus JM, Adrot O, Willison JC, Zlatev R. Modelling of hydrogen production in batch cultures of the photosynthetic bacterium *Rhodobacter capsulatus*. *Int J Hydrogen Energy* 2009;34:180–5.
 - [9] Özgür E, Uyar B, Öztürk Y, Yücel M, Gündüz U, Eroğlu I. Biohydrogen production by *Rhodobacter capsulatus* on acetate at fluctuating temperatures. *Resour Conserv Recycl* 2010;54:310–4.
 - [10] Drepper T, Groß S, Yakunin AF, Hallenbeck PC, Masepohl B, Klipp W. Role of GlnB and GlnK in ammonium control of both nitrogenase systems in the phototrophic bacterium *Rhodobacter capsulatus*. *Microbiology* 2003;149:2203–12.
 - [11] Tremblay PL, Drepper T, Masepohl B, Hallenbeck PC. Membrane sequestration of PII proteins and nitrogenase regulation in the photosynthetic bacterium *Rhodobacter capsulatus*. *J Bacteriol* 2007;189:5850–9.
 - [12] Masepohl B, Drepper T, Paschen A, Groß S, Pawlowski A, Raabe K, et al. Regulation of nitrogen fixation in the phototrophic purple bacterium *Rhodobacter capsulatus*. *J Mol Microb Biotech* 2002;4:243–8.
 - [13] Masepohl B, Klipp W. Organization and regulation of genes encoding the molybdenum nitrogenase and the alternative nitrogenase in *Rhodobacter capsulatus*. *Arch Microbiol* 1996;165:80–90.
 - [14] Liu Y, Hallenbeck PC. A kinetic study of hydrogen production by a Calvin-Benson-Bassham cycle mutant, PRK (phosphoribulose kinase), of the photosynthetic bacterium *Rhodobacter capsulatus*. *Int J Hydrogen Energy* 2016;41:11081–9.
 - [15] Tichi MA, Tabita FR. Maintenance and control of redox poise in *Rhodobacter capsulatus* strains deficient in the Calvin-Benson-Bassham pathway. *Arch Microbiol* 2000;174:322–33.
 - [16] Gökçe A, Öztürk Y, Çakar ZP, Yücel M. Temperature resistant mutants of *Rhodobacter capsulatus* generated by a directed evolution approach and effects of temperature resistance on hydrogen production. *Int J Hydrogen Energy* 2012;37:16466–72.
 - [17] Uyar B, Kapucu N. Passive temperature control of an outdoor photobioreactor by phase change materials. *J Chem Technol Biotechnol* 2015;90:915–20.
 - [18] Deatherage DE, Barrick JE. Identification of mutations in laboratory evolved microbes from next-generation sequencing data using *breseq*. *Methods Mol Biol* 2014;1151:165–88.
 - [19] Gokce A, Cakar ZP, Yucel M, Ozcan O, Sencan S, Sertdemir I, et al. Draft genome sequences of two heat-resistant mutant strains (A52 and B41) of the photosynthetic hydrogen-producing bacterium *Rhodobacter capsulatus*. *Genome Announc* 2016;4(3). <http://dx.doi.org/10.1128/genomeA.00531-16>. e00531–16.
 - [20] Hellemans J, Mortier G, De Paepe A, Speleman F, Vandesompele J. qBase relative quantification framework and software for management and automated analysis of real-time quantitative PCR data. *Genome Biol* 2007;8:R19. <http://dx.doi.org/10.1186/gb-2007-8-2-r19>. Available from: <http://genomebiology.com/2007/8/2/R19>.
 - [21] Halbleib CM, Ludden PW. Regulation of biological nitrogen fixation. *J Nutr* 2000;130:1081–4.
 - [22] Ragsdale SW. Pyruvate ferredoxin oxidoreductase and its radical intermediate. *Chem Rev* 2003;103:2333–46.
 - [23] Yakunin AF, Hallenbeck PC. Purification and characterization of pyruvate oxidoreductase from the photosynthetic bacterium *Rhodobacter capsulatus*. *BBA Bioenergetics* 1998;1409:39–49.
 - [24] Perlova O, Nawroth R, Zellermann EM, Meletzus D. Isolation and characterization of the *glnD* gene of *Gluconacetobacter diazotrophicus*, encoding a putative uridylyltransferase/uridylyl-removing enzyme. *Gene* 2002;297:159–68.
 - [25] Ninfa AJ, Jiang P. PII signal transduction proteins: sensors of α -ketoglutarate that regulate nitrogen metabolism. *Curr Opin Microbiol* 2005;8:168–73.
 - [26] Zhang Y, Pohlmann EL, Serate J, Conrad MC, Roberts GP. Mutagenesis and functional characterization of the four domains of GlnD, a bifunctional nitrogen sensor protein. *J Bacteriol* 2010;192:2711–21.
 - [27] Dos Santos PC, Dean DR, Hu Y, Ribbe MW. Formation and insertion of the nitrogenase iron-molybdenum cofactor. *Chem Rev* 2004;104:1159–74.
 - [28] Hawkes TR, Smith BE. Purification and characterization of the inactive MoFe protein (NifB-Kp1) of the nitrogenase from *nifB* mutants of *Klebsiella pneumoniae*. *Biochem J* 1983;209:43–50.
 - [29] De Smet L, Savvides SN, Van Horen E, Pettigrew G, Van Beeumen JJ. Structural and mutagenesis studies on the cytochrome c peroxidase from *Rhodobacter capsulatus* provide new insights into structure-function relationships of bacterial di-heme peroxidases. *J Biol Chem* 2006;281:4371–9.
 - [30] Turner S, Eleanor RE, Smith H, Jeffrey CO. A novel cytochrome c peroxidase from *Neisseria gonorrhoeae*: a lipoprotein from a Gram-negative bacterium. *Biochem J* 2003;373:865–73.
 - [31] Volkov AN, Nicholls P, Worrall JA. The complex of cytochrome c and cytochrome c peroxidase: the end of the road? *BBA Bioenergetics* 2011;1807:1482–503.
 - [32] Öztürk Y, Gökçe A, Peksel B, Gürkan M, Özgür E, Gündüz U, et al. Hydrogen production properties of *Rhodobacter capsulatus* with genetically modified redox balancing pathways. *Int J Hydrogen Energy* 2012;37:2014–20.
 - [33] Dangel AW, Tabita FR. CbbR, the master regulator for microbial carbon dioxide fixation. *J Bacteriol* 2015;197:3488–98.
 - [34] Van Keulen G, Girbal L, Van Den Bergh ER, Dijkhuizen L, Meijer WG. The LysR-type transcriptional regulator CbbR controlling autotrophic CO₂ fixation by *Xanthobacter flavus* is an NADPH sensor. *J Bacteriol* 1998;180:1411–7.
 - [35] Du L, Stejskal F, Tibelius KH. Characterization of two genes (*hupD* and *hupE*) required for hydrogenase activity in *Azotobacter chroococcum*. *FEMS Microbiol Lett* 1992;96:93–101.
 - [36] Curatti L, Hernandez JA, Igarashi RY, Soboh B, Zhao D, Rubio LM. In vitro synthesis of the iron-molybdenum cofactor of nitrogenase from iron, sulfur, molybdenum, and homocitrate using purified proteins. *P Natl Acad Sci USA* 2007;104:17626–31.

- [37] Jouanneau Y, Jeong HS, Hugo N, Meyer C, Willison JC. Overexpression in *Escherichia coli* of the *mif* genes from *Rhodobacter capsulatus*. *Eur J Biochem* 1998;251:54–64.
- [38] Jeong HS, Jouanneau Y. Enhanced nitrogenase activity in strains of *Rhodobacter capsulatus* that overexpress the *mif* genes. *J Bacteriol* 2000;182:1208–14.
- [39] Bertsova YV, Fadeeva MS, Kostyrko VA, Serebryakova MV, Baykov AA, Bogachev AV. Alternative pyrimidine biosynthesis protein ApbE is a flavin transferase catalyzing covalent attachment of FMN to a threonine residue in bacterial flavoproteins. *J Biol Chem* 2013;288:14276–86.
- [40] Hayashi NR, Arai H, Kodama T, Igarashi Y. The novel genes, *cbbQ* and *cbbO*, located downstream from the *RubisCO* genes of *Pseudomonas hydrogenothermophila*, affect the conformational states and activity of *RubisCO*. *Biochem Biophys Res Commun* 1997;241:565–9.
- [41] Tsai YC, Lapina MC, Bhushan S, Mueller-Cajar O. Identification and characterization of multiple *RubisCO* activases in chemoautotrophic bacteria. *Nat Commun* 2015;6:8883. <http://dx.doi.org/10.1038/ncomms9883>.
- [42] Schüddekopf K, Hennecke S, Liese U, Kutsche M, Klipp W. Characterization of *anf* genes specific for the alternative nitrogenase and identification of *nif* genes required for both nitrogenases in *Rhodobacter capsulatus*. *Mol Microbiol* 1993;8:673–84.
- [43] Neumann M, Stöcklein W, Leimkühler S. Transfer of the molybdenum cofactor synthesized by *Rhodobacter capsulatus* MoeA to XdhC and MobA. *J Biol Chem* 2007;282:28493–500.
- [44] Dixon R, Kahn D. Genetic regulation of biological nitrogen fixation. *Nat Rev Microbiol* 2004;2:621–31.
- [45] Arcondéguy T, Jack R, Merrick M. PII signal transduction proteins, pivotal players in microbial nitrogen control. *Microbiol Mol Biol Rev* 2001;65:80–105.
- [46] Wang D, Zhang Y, Welch E, Li J, Roberts GP. Elimination of *RubisCO* alters the regulation of nitrogenase activity and increases hydrogen production in *Rhodospirillum rubrum*. *Int J Hydrogen Energy* 2010;35:7377–85.